

Copyright © 1993, by the author(s).
All rights reserved.

Permission to make digital or hard copies of all or part of this work for personal or classroom use is granted without fee provided that copies are not made or distributed for profit or commercial advantage and that copies bear this notice and the full citation on the first page. To copy otherwise, to republish, to post on servers or to redistribute to lists, requires prior specific permission.

**CONTROL STRATEGIES FOR MOBILE ROBOTS
WITH TRAILERS**

by

D. Tilbury, J-P. Laumond, R. Murray, S. Sastry,
and G. Walsh

Memorandum No. UCB/ERL M93/23

12 March 1993

**CONTROL STRATEGIES FOR MOBILE ROBOTS
WITH TRAILERS**

by

D. Tilbury, J-P. Laumond, R. Murray, S. Sastry,
and G. Walsh

Memorandum No. UCB/ERL M93/23

12 March 1993

ELECTRONICS RESEARCH LABORATORY

College of Engineering
University of California, Berkeley
94720

TITLE PAGE

**CONTROL STRATEGIES FOR MOBILE ROBOTS
WITH TRAILERS**

by

D. Tilbury, J-P. Laumond, R. Murray, S. Sastry,
and G. Walsh

Memorandum No. UCB/ERL M93/23

12 March 1993

ELECTRONICS RESEARCH LABORATORY

College of Engineering
University of California, Berkeley
94720

Control Strategies for Mobile Robots with Trailers*

D. Tilbury, J-P. Laumond[†], R. Murray[‡], S. Sastry, G. Walsh

Electronics Research Laboratory
Department of Electrical Engineering and Computer Science
University of California Berkeley, CA 94720

Abstract

In this paper we propose two open-loop control schemes for planning feasible paths for a mobile robot with trailers. Both methods use sinusoidal inputs. The first method uses sinusoids at integrally related frequencies for systems in so-called chained form. This method is simple, however, it only applies to mobile robots with one trailer and it makes no provision for obstacle avoidance. The second method is very general in that it can be applied to systems which may not be convertible to chained form. An initial path through the state space is generated using well-known techniques from the literature (this path can be chosen to avoid obstacles if desired), then a feasible path is constructed which follows this nominal path arbitrarily closely. This method, however, uses inputs of arbitrarily high amplitude and high frequency. We study the connections between the two methods. We also discuss the importance of coordinates, since the first of our methods will only work on systems that can be put into "chained" coordinates, and the tracking results of the second method are shown to depend upon the coordinate system in which the equations are expressed. We show that our system can be converted into an approximate chained form, and that the asymptotic sinusoids method works better in these coordinates. Finally, simulation results for a mobile robot with two trailers are presented.

1 Introduction

This paper investigates methods for planning collision-free paths for a mobile robot with trailers, a popular and perhaps canonical example of a Nonholonomic Motion Planning problem.

The Nonholonomic Motion Planning problem concerns motion planning for systems which have fewer degrees of freedom than configuration parameters. For example, simple mobile robots with wheels generally have two degrees of freedom (linear and rotational velocities) and three parameters to be controlled (two position parameters and one orientation parameter). While the classical tools in (holonomic) motion planning come from computational and algebraic geometry (see [10]), the nonholonomic motion planning problem demands the use of tools developed in nonlinear geometric control theory (see the pioneering works [15, 17, 18], and [16] for an overview).

*Research supported in part by NSF grant IRI90-14450

[†]Address: Laboratoire d'Automatique et d'Analyse des Systèmes, 31077 Toulouse CEDEX, France

[‡]Current Address: Department of Mechanical Engineering, California Institute of Technology, Pasadena, CA 91125

The two types of constraints that will interest us in planning for mobile robots are position constraints and velocity constraints. The position constraints generally arise from obstacles in the configuration space, and can be expressed directly as limits on the allowable configurations of the system. The velocity constraints, however, are expressed as constraints on the tangent space to the configuration space. They will limit the directions in which the system can move at any point, however, they do not necessarily reduce the reachable configuration space. In the case of r linked bodies corresponding to r equations linear in the derivatives of the n configuration parameters, these constraint equations determine what is called an $(n - r)$ -distribution Δ on the configuration manifold. According to Frobenius' theorem (see for instance [22]), the equations are integrable if and only if the distribution Δ is closed under the Lie bracket operation¹. If the equations are integrable the constraints are said to be holonomic and the system will be forced to move inside a sub-manifold of the configuration space. If the equations are not integrable, the system is said to be nonholonomic. In this case, the main question is : do the constraints reduce the *accessible* configuration space ?

The answer to this question is given by the controllability theorem for non-linear systems (see for instance [26, 6]). The control Lie algebra associated with the distribution Δ , denoted by $LA(\Delta)$, is the smallest distribution which contains Δ and is closed under the Lie bracket operation. If the Lie algebra has full rank at a given configuration point c , then for any neighborhood \mathcal{N}' of c , there exists a neighborhood \mathcal{N} of c whose points represent reachable configurations for the system moving from c along an admissible path lying in \mathcal{N}' . This condition is known as the "rank condition"; it is a *local* condition. If the rank condition holds everywhere in the configuration space, then the system is termed *controllable*. From the planning point of view, the main consequence is that the existence of a collision-free path is characterized by the existence of a connected component in the *free* (i.e., with neither collision nor contact) configuration space.

Therefore the decision problem of motion planning, that is, deciding whether or not a feasible path exists, for controllable nonholonomic systems is the same as that for holonomic ones: the start and goal positions must lie in the same connected component of the free configuration space.

The difference lies with the complete problem, since the controllability result is not constructive. At this stage we could hope that the search for a solution to a nonholonomic system can be guided by a collision-free path for the associated holonomic system. Indeed, thanks to the local property above, a controllable robot can be steered close to any path as long as there is a "small gap" between the reference path and the obstacles². This idea has been refined into two different approaches. The first one developed in [21] uses an explicit form of the shortest paths in order to approximate any holonomic path of a car-like system. The second one uses sinusoidal inputs in order to compute such approximations for some canonical systems [18] and general ones [24]. In this paper, we investigate this second approach for the case of a mobile robot with trailers.

The paper is organized as follows. We first give a brief description of a mobile robot system and derive the kinematic equations that the system obeys. We also demonstrate explicitly that the system is completely controllable. A coordinate change transforming the system of the mobile robot with one trailer, into a special "chained canonical form" is presented. Systems in this form can be steered using Murray and Sastry's sinusoidal algorithm. We propose a new set of coordinates for the two-trailer system corresponding to an approximate chained form.

A method originally proposed by Sussmann and Liu is used to generate a sequence of paths

¹Let us recall that the Lie bracket of two vector fields X and Y is defined as $[X, Y] = \partial X.Y - \partial Y.X$.

²See [14] for these topological aspects.

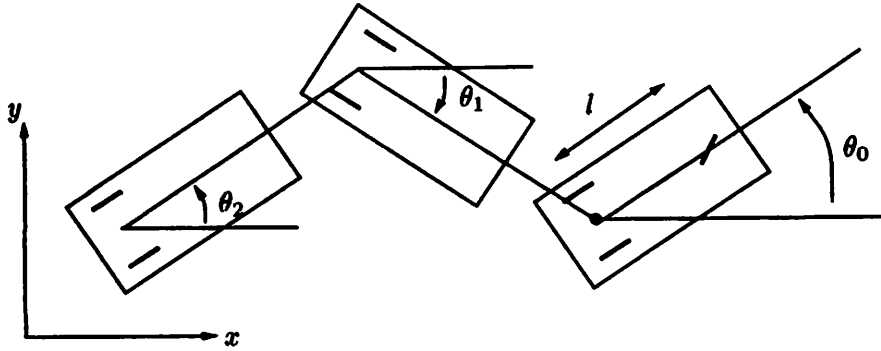


Figure 1: The mobile robot Hilare with 2 trailers.

for the two trailer system which converge to any desired trajectory. We show simulation results demonstrating this convergence, and note the improved convergence results obtained with the approximate chained form coordinates for certain desired paths.

2 The Two-trailer System

Consider a mobile robot such as Hilare³ with two trailers attached, as in Figure 1. Each trailer is attached to the body in front of it by a rigid bar, and the rear set of wheels of each body is constrained to roll without slipping. The trailers are assumed to be identical, and to have a link length of l . The connections between the bodies give rise to the following constraints:

$$\begin{aligned} x_i &= x_{i-1} - l \cos \theta_i \\ y_i &= y_{i-1} - l \sin \theta_i \end{aligned} \quad (1)$$

$i = 1, 2, \dots, n$ for the general n -trailer case. These constraints are integrable and will reduce the dimension of the configuration space, since the positions (x_i, y_i) for $i \geq 1$ can be expressed in terms of $x_0, y_0, \theta_0, \dots, \theta_i$. The position and orientation of all the bodies can be specified by the $n + 3$ variables $(x_0, y_0, \theta_0, \theta_1, \dots, \theta_n)$. We will take the length of each link to be one unit, *i.e.* $l = 1$. We have assumed that the bodies are connected between the midpoints of the two sets of rear wheels; it should be noted that if the trailers are hitched behind the rear axle, the equations will not simplify as shown here.

We assume that the wheels of the robot and trailers roll without slipping; this implies that the velocity of each body in the direction perpendicular to its wheels must be zero. We model each pair of rear wheels as a single wheel at the midpoint of the axle, and state the non-slipping conditions in terms of coordinates as:

$$0 = \dot{x}_i \sin \theta_i - \dot{y}_i \cos \theta_i$$

Using the connection relations between the bodies (1), these three constraints become (for the two-trailer system):

$$0 = \dot{x}_0 \sin \theta_0 - \dot{y}_0 \cos \theta_0$$

³The Hilare family of mobile robots resides at LAAS in Toulouse, see for example [3, 4].

$$\begin{aligned}
0 &= \dot{x}_0 \sin \theta_1 - \dot{y}_0 \cos \theta_1 + \dot{\theta}_1 \\
0 &= \dot{x}_0 \sin \theta_2 - \dot{y}_0 \cos \theta_2 + \cos(\theta_1 - \theta_2)\dot{\theta}_1 + \dot{\theta}_2
\end{aligned}$$

These non-slipping constraints on the velocities of the system are nonholonomic, or nonintegrable. They can be written more compactly as $\omega(x) \cdot \dot{x} = 0$ for the state vector $x = (x_0, y_0, \theta_0, \theta_1, \theta_2)$ and the following one-forms on $Q = \mathbf{R}^2 \times S^1 \times S^1 \times S^1$:

$$\begin{aligned}
\omega_1(x) &= [\sin \theta_0 & -\cos \theta_0 & 0 & 0 & 0] \\
\omega_2(x) &= [\sin \theta_1 & -\cos \theta_1 & 0 & 1 & 0] \\
\omega_3(x) &= [\sin \theta_2 & -\cos \theta_2 & 0 & \cos(\theta_1 - \theta_2) & 1]
\end{aligned}$$

The co-distribution $\Omega(x) = \text{span}\{\omega_1(x), \omega_2(x), \omega_3(x)\}$ has dimension three and the state space Q is of dimension five, so there exists a two-dimensional distribution $\Delta(x) = \text{span}\{g_1(x), g_2(x)\}$ such that $\Delta = \Omega^\perp$, i.e.,

$$\omega(x) \cdot g(x) = 0, \quad \forall \omega \in \Omega, \forall g \in \Delta$$

A simple calculation will show that the following vector fields g_1, g_2 form a basis for Δ :

$$g_1 = \begin{pmatrix} \cos \theta_0 \\ \sin \theta_0 \\ 0 \\ \sin(\theta_0 - \theta_1) \\ \sin(\theta_1 - \theta_2) \cos(\theta_0 - \theta_1) \end{pmatrix} \quad g_2 = \begin{pmatrix} 0 \\ 0 \\ 1 \\ 0 \\ 0 \end{pmatrix} \quad (2)$$

We can therefore formulate the mobile robot with two trailers as a control system,

$$\dot{x} = g_1(x)u_1 + g_2(x)u_2 \quad (3)$$

with the state $x = (x_0, y_0, \theta_0, \theta_1, \theta_2)$ and the input vector fields g_1 and g_2 as defined above. This is the dual representation of the constraints: the forms $\omega(x)$ represent the constraints on the velocities, and the vector fields g_i represent the allowable velocities of the system. The two control inputs correspond to the two instantaneous degrees of freedom for the system: u_1 , the driving velocity of the lead car, and u_2 , the steering velocity of the front wheel.

The problem of finding a feasible path between one configuration and another can be reformulated as a control problem: find inputs $u_1(t), u_2(t)$ which will steer the system from an initial state x^o to a final state x^f .

We recall the result from control theory [7] which states that a system of the form (3) is *completely controllable*, that is, given any $x^o, x^f \in Q$, there exists a time T and an input $u(\cdot) : [0, T] \rightarrow \mathbf{R}^2$ which steers the system from state x^o at time 0 to state x^f at time T , if the smallest involutive distribution containing the input vector fields spans the tangent space to the configuration space, i.e. system (3) is completely controllable if

$$\text{inv}(G) = \text{inv}(\text{span}\{g_1, g_2\}) = TQ \quad (4)$$

To form $\text{inv}(G)$ we add to the distribution G the Lie brackets of its elements

$$\text{inv}(G) = \{g_1, g_2, [g_1, g_2], [g_1, [g_1, g_2]], [g_2, [g_1, g_2]], \dots\}$$

The existence of five linearly independent vector fields in $\text{inv}(G)$ will imply $\text{inv}(G) = TQ$ and thus complete controllability.

To simplify the notation somewhat, we define the vector fields g_3, g_4, g_5, g_6 as follows:

$$\begin{aligned} g_3 &= [g_1, g_2] \\ g_4 &= [g_1, [g_1, g_2]] \\ g_5 &= [g_1, [g_1, [g_1, g_2]]] \\ g_6 &= [g_1, [g_1, [g_1, [g_1, g_2]]]] \end{aligned} \quad (5)$$

These vector fields have the following form: $\{g_1, g_2, g_3, g_4, g_5, g_6\} =$

$$\begin{aligned} &\begin{pmatrix} \cos \theta_0 \\ \sin \theta_0 \\ 0 \\ \sin(\theta_0 - \theta_1) \\ \cos(\theta_0 - \theta_1) - \sin(\theta_1 - \theta_2) \end{pmatrix}, \begin{pmatrix} 0 \\ 0 \\ 1 \\ 0 \\ 0 \end{pmatrix}, \begin{pmatrix} \sin \theta_0 \\ -\cos \theta_0 \\ 0 \\ -\cos(\theta_0 - \theta_1) \\ \sin(\theta_0 - \theta_1) \sin(\theta_1 - \theta_2) \end{pmatrix}, \begin{pmatrix} 0 \\ 0 \\ 0 \\ -1 \\ \cos(\theta_1 - \theta_2) \end{pmatrix}, \\ &\begin{pmatrix} 0 \\ 0 \\ 0 \\ -\cos(\theta_0 - \theta_1) \\ \cos(\theta_0 - \theta_1)[1 + \cos(\theta_1 - \theta_2)] \end{pmatrix}, \begin{pmatrix} 0 \\ 0 \\ 0 \\ -1 \\ 1 + \cos(\theta_1 - \theta_2)[1 + \cos^2(\theta_0 - \theta_1)] \end{pmatrix} \end{aligned}$$

The vector fields $\{g_1, \dots, g_5\}$ are linearly independent on an open set

$$U = \{(x_0, y_0, \theta_0, \theta_1, \theta_2) : \theta_0 - \theta_1 \neq \pm \frac{\pi}{2}\}.$$

This can be checked by finding the determinant of the 5×5 matrix whose columns are the g_i 's:

$$\det \begin{bmatrix} | & | & | & | & | \\ g_1 & g_2 & g_3 & g_4 & g_5 \\ | & | & | & | & | \end{bmatrix} = \cos(\theta_0 - \theta_1)$$

When this matrix has a nonzero determinant, it is full rank and its columns are linearly independent. On the set $U' = Q - U = \{(x_0, y_0, \theta_0, \theta_1, \theta_2) : \theta_0 - \theta_1 = \pm \frac{\pi}{2}\}$, the vector field $g_5(x^0) \equiv 0$. Consider in its place the vector field g_6 . The five vector fields $\{g_1, g_2, g_3, g_4, g_6\}$ are linearly independent on U' ; again, we check linear independence by taking the determinant of the following matrix:

$$\det \begin{bmatrix} | & | & | & | & | \\ g_1 & g_2 & g_3 & g_4 & g_6 \\ | & | & | & | & | \end{bmatrix} = -1 - \cos^2(\theta_0 - \theta_1) \cos(\theta_1 - \theta_2) = -1, \quad \forall x \in U'$$

Thus we have shown that at every point $x \in Q$, $\text{inv}(G) = T_x Q$ and therefore the two-trailer system is completely controllable.

The input vector fields for the one-trailer system are truncated versions of those for the two-trailer system shown above, and controllability of this system is checked in exactly the same manner. It can be shown that the general n -trailer system is also completely controllable; see Laumond [13] for details.

Complete controllability implies that there exists a feasible path (a path satisfying the velocity constraints) between any two points in the configuration space. The problem that we consider is that of finding such a path.

3 Steering Systems in Chained Form

We digress slightly here to present an algorithm for steering systems which are in “chained canonical form.” Although this special form may seem somewhat restrictive at first glance, we will show how many systems can be put into this form using state feedback and an input transformation, and then steered using a simple algorithm which we also describe here.

Consider a two-input control system of the form

$$\dot{x} = g_1(x)u_1 + g_2(x)u_2$$

where the state $x = (x_1, \dots, x_n)^T$ and the input vector fields have the following very special form:

$$g_1 = \begin{pmatrix} 1 \\ 0 \\ x_2 \\ x_3 \\ \vdots \\ x_{n-2} \end{pmatrix} \quad g_2 = \begin{pmatrix} 0 \\ 1 \\ 0 \\ 0 \\ \vdots \\ 0 \end{pmatrix} \quad (6)$$

It can be shown that systems of this form are completely controllable; and we outline here an algorithm for steering. Given an initial state x^o and a desired final state x^f , choose a period T and find the corresponding frequency $\omega = \frac{2\pi}{T}$.

Algorithm 1 (Step-by-step Steering with Sinusoids [19])

STEP 0. Set the inputs to be constant over the time interval $[0, T]$,

$$u_1 = \frac{1}{T}(x_1^f - x_1^o)$$

$$u_2 = \frac{1}{T}(x_2^f - x_2^o)$$

This will drive x_1 and x_2 to their desired final positions.

STEP 1. Over the time interval $[T, 2T]$, set the inputs to be

$$u_1 = \alpha \sin \omega t$$

$$u_2 = \beta \cos \omega t$$

where α and β are chosen such that

$$x_3^f - x_3(T) = \frac{\alpha\beta}{2\omega}T$$

After this step, $x_3(2T) = x_3^f$ its desired final value, and

$$x_1(2T) = x_1(T) = x_1^f \text{ and } x_2(2T) = x_2(T) = x_2^f$$

are also at their desired final values.

STEP k . ($k = 2, \dots, n - 2$)

Over the time interval $[kT, (k + 1)T]$, set the inputs to be

$$u_1 = \alpha \sin \omega t$$

$$u_2 = \beta \cos k\omega t$$

where α and β are chosen such that

$$x_{k+2}^f - x_{k+2}(kT) = \frac{\alpha^k \beta}{(2\omega)^k k!} T$$

After Step k , states x_1, x_2, \dots, x_{k+2} are in their desired final positions.

For $x \in \mathbf{R}^n$, the total steering time is $(n - 2)T$. The required time can be reduced by initially choosing a smaller value of T .

Remark. Instead of steering each state separately, we could choose inputs of the form:

$$\begin{aligned} u_1 &= \alpha_0 + \alpha_1 \sin \omega_1 t + \alpha_2 \sin \omega_2 t + \cdots + \alpha_{n-2} \sin \omega_{n-2} t \\ u_2 &= \beta_0 + \beta_1 \cos \omega_1 t + \beta_2 \cos 2\omega_2 t + \cdots + \beta_{n-2} \cos(n-2)\omega_{n-2} t \end{aligned}$$

over the time interval $[0, T]$ where T is a multiple of the periods corresponding to each ω_i , i.e. there exist integers k_i such that $T = k_i \frac{2\pi}{\omega_i}$, $i = 1, \dots, n-2$. However, the computation required to find the coefficients α_i, β_i is much more complex. For example, in the four-state chained form:

$$\begin{aligned} \dot{x}_1 &= u_1 \\ \dot{x}_2 &= u_2 \\ \dot{x}_3 &= x_2 u_1 \\ \dot{x}_4 &= x_3 u_1 \end{aligned}$$

the inputs would be of the form:

$$\begin{aligned} u_1 &= \alpha_0 + \alpha_1 \sin \omega_1 t + \alpha_2 \sin \omega_2 t \\ u_2 &= \beta_0 + \beta_1 \cos \omega_1 t + \beta_2 \cos 2\omega_2 t \end{aligned}$$

and after one period T , the states would be:

$$\begin{aligned} x_1(T) &= x_1^o + \alpha_0 T \\ x_2(T) &= x_2^o + \beta_0 T \\ x_3(T) &= x_3^o + \frac{\alpha_1 \beta_1}{2\omega_1} T + \alpha_0 x_2^o T + \frac{\alpha_0 \beta_0}{2} T^2 - \frac{\alpha_1 \beta_0}{\omega_1} T - \frac{\alpha_2 \beta_0}{\omega_2} T \\ x_4(T) &= x_4^o + \frac{\alpha_2^2 \beta_2}{8\omega_2^2} T + \alpha_0 x_3^o T + \frac{\alpha_0^2 x_2^o}{2} T^2 + \frac{\alpha_0^2 \beta_0}{6} T^3 + \frac{\alpha_1 \alpha_2 \beta_0}{\omega_1 \omega_2} T - \frac{\alpha_1 \alpha_2 \beta_1}{2\omega_1 \omega_2} T \\ &\quad + \frac{\alpha_0 \alpha_1 \beta_1}{4\omega_1} T^2 - \frac{\alpha_0 \alpha_1 \beta_0}{2\omega_1} T^2 - \frac{\alpha_0 \alpha_2 \beta_0}{2\omega_2} T^2 + \frac{3\alpha_1^2 \beta_0}{4\omega_1^2} T + \frac{3\alpha_2^2 \beta_0}{4\omega_2^2} T \\ &\quad + \frac{\alpha_0^2 \beta_1}{\omega_1^2} T + \frac{\alpha_0^2 \beta_2}{4\omega_2^2} T - \frac{\alpha_1^2 \beta_1}{2\omega_1^2} T \end{aligned}$$

and there are certain noninterference conditions between the two frequencies that must be satisfied, namely:

$$\begin{aligned} \omega_1 &\neq \pm \omega_2 \\ \omega_1 &\neq \pm 2\omega_2 \\ \omega_1 &\neq \pm 3\omega_2 \end{aligned}$$

Since the two frequencies must have a common period, we could choose a combination such as $2\omega_1 = \omega_2$ or $2\omega_1 = 3\omega_2$, or more generally, $q\omega_1 = p\omega_2$, $\frac{p}{q} \neq 1, 2, 3$.

The equations that need to be solved to find the coefficients α_i, β_i are more complex for the general n -state case, but there are more degrees of freedom in choosing the amplitude coefficients than there are constraints on the final values of $x_i(T)$, and so it is possible to choose these coefficients and use this method of steering. The advantage of the step-by-step method of Algorithm 1 is the ease of presentation and implementation.

Although the steering procedure presented above is useful only for systems in chained canonical form, many systems can be put into this form through a coordinate change and state feedback. A set of sufficient conditions for such a transformation to exist is detailed in [19]. These conditions are not satisfied for all systems, including the two-trailer mobile robot system which we consider in this paper. Therefore, we state a generalization of the transformation proposition, using a relaxed set of conditions which are sufficient for putting a system into an approximate chained form.

Proposition 1 (Transformation to Approximate Chained Form.)

Consider a two-input control system

$$\dot{x} = g_1(x)u_1 + g_2(x)u_2$$

with g_1, g_2 having the following special form on an open set:

$$g_1(x) = \frac{\partial}{\partial x_1} + \sum_{i=2}^n g_1^i \frac{\partial}{\partial x_i}$$

$$g_2(x) = \sum_{i=2}^n g_2^i \frac{\partial}{\partial x_i}$$

Consider some order- ρ approximation of the input vector fields, \tilde{g}_1 and \tilde{g}_2 , where⁴

$$g_1(x) = \tilde{g}_1(x) + O(x)^{\rho+1}$$

$$g_2(x) = \tilde{g}_2(x) + O(x)^{\rho+1}$$

Define the distributions

$$\Delta_0 = \text{span}\{\tilde{g}_1, \tilde{g}_2, \text{ad}_{\tilde{g}_1}\tilde{g}_2, \dots, \text{ad}_{\tilde{g}_1}^{n-2}\tilde{g}_2\}$$

$$\Delta_1 = \text{span}\{\tilde{g}_2, \text{ad}_{\tilde{g}_1}\tilde{g}_2, \dots, \text{ad}_{\tilde{g}_1}^{n-3}\tilde{g}_2\}$$

If for some open set U , $\Delta_0(x) = T_x Q$ for all $x \in U$ and Δ_1 is involutive on U , then there exists a local feedback transformation on U :

$$\xi = \phi(x)$$

$$u = \beta(x)v$$

such that the transformed system is in order- ρ chained form, that is:

$$\begin{aligned} \dot{\xi}_1 &= v_1 \\ \dot{\xi}_2 &= v_2 \\ \dot{\xi}_3 &= \xi_2 v_1 + O(\xi)^{\rho+1} \\ &\vdots \\ \dot{\xi}_n &= \xi_{n-1} v_1 + O(\xi)^{\rho+1} \end{aligned} \tag{7}$$

⁴Here and in what follows, $O(x)^\rho$ means terms that are of order ρ or higher in x ; more precisely, $f(x)$ is of order ρ in x , or $O(x)^\rho$, if:

$$\lim_{x \rightarrow 0} \frac{\|f(x)\|}{\|x\|^\rho} = M, \quad |M| < \infty$$

Proof: (by construction). Consider first a distribution $\Delta' = \text{span}\{\tilde{g}_2, \text{ad}_{\tilde{g}_1}\tilde{g}_2, \dots, \text{ad}_{\tilde{g}_1}^{n-2}\tilde{g}_2\}$. From the special form of the input vector fields, it can be seen that none of the vector fields in Δ' have a component $\frac{\partial}{\partial x_1}$. Since Δ_0 has rank n , Δ' must have rank $n - 1$, and Δ' is involutive because of this special form.

Now, Δ_1 is involutive and of dimension $n - 2$, so there exists a function $h : U \rightarrow \mathbf{R}$ such that

$$\begin{aligned} dh \cdot \Delta_1 &= 0 \\ dh \cdot \text{ad}_{\tilde{g}_1}^{n-2}\tilde{g}_2 &= a(x) \end{aligned}$$

where the function $a(x)$ is bounded away from zero on U . We define the coordinate transformation $\phi : x \mapsto \xi$ as

$$\begin{aligned} \xi_1 &= x_1 \\ \xi_2 &= L_{\tilde{g}_1}^{n-2}h \\ &\vdots \\ \xi_{n-1} &= L_{\tilde{g}_1}h \\ \xi_n &= h \end{aligned} \tag{8}$$

The Lie derivative that we have used in the definition of this coordinate change is defined as follows: for a function $h : Q \rightarrow \mathbf{R}$ and a vector field $g(x)$ on Q , the derivative of h along g is $L_g h(x) = dh(x) \cdot g(x)$. We denote repeated Lie derivatives by:

$$L_g^k h(x) = d(L_g^{k-1}h(x)) \cdot g(x)$$

where the zeroth Lie derivative is defined as $L_g^0 h(x) = h(x)$.

To verify that 8 is a valid change of coordinates, we calculate its Jacobean with respect to x and show that it is nonsingular:

$$\frac{\partial \phi}{\partial x} = \begin{bmatrix} 1 & 0 & \dots & 0 \\ dL_{\tilde{g}_1}^{n-2}h \\ \vdots \\ dL_{\tilde{g}_1}h \\ dh \end{bmatrix}$$

We multiply $\frac{\partial \phi}{\partial x}$ on the right by the nonsingular matrix whose columns are the independent elements of Δ_0 :

$$\begin{aligned} \frac{\partial \phi}{\partial x} \cdot [\Delta_0] &= \begin{bmatrix} 1 & 0 & \dots & 0 \\ dL_{\tilde{g}_1}^{n-2}h \\ \vdots \\ dL_{\tilde{g}_1}h \\ dh \end{bmatrix} \begin{bmatrix} \tilde{g}_1 & \tilde{g}_2 & \text{ad}_{\tilde{g}_1}\tilde{g}_2 & \dots & \text{ad}_{\tilde{g}_1}^{n-2}\tilde{g}_2 \end{bmatrix} \\ &= \begin{bmatrix} 1 & 0 & 0 & \dots & 0 \\ * & \pm a(x) & * & \dots & * \\ * & 0 & \pm a(x) & & \vdots \\ \vdots & \vdots & & \ddots & * \\ * & 0 & \dots & 0 & a(x) \end{bmatrix} \end{aligned}$$

where $a(x) = dh \cdot \text{ad}_{\tilde{g}_1}^{n-2} \tilde{g}_2$ is bounded away from zero by the definition of h .

Since the resulting matrix has rank n for all $x \in U$, the two matrices $\frac{\partial \phi}{\partial x}$ and $[\Delta_0]$ must also have rank n . Thus the coordinate transform we have described in (8) is valid on the open set U .

The approximate chained form follows from the involutivity of Δ_1 . Consider the coordinate $\xi_n = h$, and its derivative:

$$\begin{aligned} \dot{\xi}_n &= (L_{g_1} h)u_1 + (L_{g_2} h)u_2 \\ &= dh \cdot (\tilde{g}_1 + O(x)^{\rho+1})u_1 + dh \cdot (\tilde{g}_2 + O(x)^{\rho+1})u_2 \\ &= (L_{\tilde{g}_1} h)u_1 + (L_{\tilde{g}_2} h)u_2 + dh \cdot O(x)^{\rho+1}(u_1 + u_2) \end{aligned}$$

Noting that $L_{\tilde{g}_1} h = \xi_{n-1}$ and that $L_{\tilde{g}_2} h = 0$, we see that

$$\dot{\xi}_n = \xi_{n-1}v_1 + O(\xi)^{\rho+1}$$

The same procedure can then be applied to ξ_{n-1}, \dots, ξ_1 , and it will be seen that the input transformation

$$\begin{aligned} v_1 &= u_1 \\ v_2 &= (L_{g_1} L_{\tilde{g}_1}^{n-2} h)u_1 + (L_{g_2} L_{\tilde{g}_1}^{n-2} h)u_2 \end{aligned}$$

is necessary for the system in transformed coordinates to be in the order- ρ chained form (7). \square

Remark. If the distribution $\Delta_0 = TQ$ and Δ_1 is involutive using the original vector fields g_1, g_2 instead of their order- ρ approximations, then the procedure above will result in a system in exact chained form.

4 Transformations to Chained Forms

For the mobile robot with one trailer, a transformation to exact chained form can be found using Proposition 1. Recall that the state is $x = (x_0, y_0, \theta_0, \theta_1)$ and the input vector fields are:

$$g_1 = \begin{pmatrix} \cos \theta_0 \\ \sin \theta_0 \\ 0 \\ \sin(\theta_0 - \theta_1) \end{pmatrix} \quad g_2 = \begin{pmatrix} 0 \\ 0 \\ 1 \\ 0 \end{pmatrix}$$

Although these are not in the form that was assumed in the statement of the theorem, we can divide g_1 by $\cos \theta_0$ (equivalent to a simple input transformation $\tilde{u}_1 = u_1 \cos \theta_0$)

$$g_1 = \begin{pmatrix} 1 \\ \tan \theta_0 \\ 0 \\ \frac{\sin(\theta_0 - \theta_1)}{\cos \theta_0} \end{pmatrix} \quad g_2 = \begin{pmatrix} 0 \\ 0 \\ 1 \\ 0 \end{pmatrix}$$

Now we form the distributions

$$\Delta_0 = \text{span} \left\{ \begin{pmatrix} 1 \\ \tan \theta_0 \\ 0 \\ \frac{\sin(\theta_0 - \theta_1)}{\cos \theta_0} \end{pmatrix}, \begin{pmatrix} 0 \\ 0 \\ 1 \\ 0 \end{pmatrix}, \begin{pmatrix} 0 \\ -\sec^2 \theta_0 \\ 0 \\ \frac{\cos \theta_1}{\cos^2 \theta_0} \end{pmatrix}, \begin{pmatrix} 0 \\ 0 \\ 0 \\ -\sec^2 \theta_0 \end{pmatrix} \right\}$$

$$\Delta_1 = \text{span} \left\{ \begin{pmatrix} 0 \\ 0 \\ 1 \\ 0 \end{pmatrix}, \begin{pmatrix} 0 \\ -\sec^2 \theta_0 \\ 0 \\ \frac{\cos \theta_1}{\cos^2 \theta_0} \end{pmatrix} \right\}$$

We note that

$$\text{rank} \Delta_0(x) = 4, \quad \forall x \in \{(x_0, y_0, \theta_0, \theta_1) : \theta_0 \neq \frac{\pi}{2}\}$$

and that Δ_1 is involutive. If we use the notation $g_3 = [g_1, g_2]$ then $\Delta_1 = \text{span}\{g_2, g_3\}$ and since

$$\begin{aligned} [g_2, g_3] &= \begin{pmatrix} 0 \\ \frac{-2 \tan \theta_0}{\cos^2 \theta_0} \\ 0 \\ \frac{2 \tan \theta_0 \cos \theta_1}{\cos^2 \theta_0} \end{pmatrix} \\ &= 2 \tan \theta_0 g_3 \\ &\in \Delta_1 \end{aligned}$$

Δ_1 is involutive. It can be seen that the function

$$\begin{aligned} h : \mathbf{R}^2 \times S^1 \times S^1 &\longrightarrow \mathbf{R} \\ h(x_0, y_0, \theta_0, \theta_1) &= y - \log \frac{1 + \sin \theta_1}{\cos \theta_1} \end{aligned}$$

will satisfy the conditions

$$\begin{aligned} dh \cdot \Delta_1 &= 0 \\ dh \cdot [g_1, [g_1, g_2]] &\neq 0 \end{aligned}$$

We can now follow the steps given in Proposition 1 for finding the coordinate transformation

$$\begin{aligned} \xi_1 &= x_0 \\ \xi_2 &= L_{g_1}^2 h = \frac{\cos(\theta_0 - \theta_1) \sin(\theta_0 - \theta_1) - \tan \theta_1 \sin^2(\theta_0 - \theta_1)}{\cos^2 \theta_0 \cos \theta_1} \\ \xi_3 &= L_{g_1} h = \tan \theta_0 - \frac{\sin(\theta_0 - \theta_1)}{\cos \theta_0 \cos \theta_1} \\ \xi_4 &= h = y - \log \frac{1 + \sin \theta_1}{\cos \theta_1} \end{aligned}$$

There is also a corresponding input transformation (state feedback),

$$\begin{aligned} v_1 &= u_1 \\ v_2 &= -\frac{\cos^2(\theta_0 - \theta_1) \sin(\theta_0 - \theta_1)}{\cos^3 \theta_0 \cos \theta_1} u_1 + \frac{3 \sin^2 \theta_1 \cos(\theta_0 - \theta_1) \sin^2(\theta_0 - \theta_1)}{2 \cos^3 \theta_0 \cos^3 \theta_1} u_1 \\ &\quad - \frac{2 \sin^2 \theta_1 \sin^3(\theta_1 - \theta_0)}{\cos^3 \theta_0 \cos^3 \theta_1} u_1 + \frac{1}{\cos^2 \theta_0 \cos \theta_1} u_2 \end{aligned}$$

and the system equations in the new coordinates are in chained canonical form

$$\begin{aligned}\dot{\xi}_1 &= v_1 \\ \dot{\xi}_2 &= v_2 \\ \dot{\xi}_3 &= \xi_2 v_1 \\ \dot{\xi}_4 &= \xi_3 v_1\end{aligned}$$

The step-by-step sinusoids method described in Algorithm 1 can now be used to steer this system from any initial condition to any desired final position.

For the two-trailer system consisting of the car-like robot with two trailers, the conditions of Proposition 1 are satisfied only for $\rho = 1$. We show here the transformation to approximate (order-1) chained form.

We recall that the equations for this system are of the form

$$\dot{x} = g_1(x)u_1 + g_2(x)u_2$$

where the state vector $x = (x_0, y_0, \theta_0, \theta_1, \theta_2)$ and the input vector fields are

$$g_1 = \begin{pmatrix} \cos \theta_0 \\ \sin \theta_0 \\ 0 \\ \sin(\theta_0 - \theta_1) \\ \cos(\theta_0 - \theta_1) \sin(\theta_1 - \theta_2) \end{pmatrix} \quad g_2 = \begin{pmatrix} 0 \\ 0 \\ 1 \\ 0 \\ 0 \end{pmatrix}$$

Using the Taylor expansion for the sine and cosine functions up to terms of order 1,

$$\begin{aligned}\sin \alpha &= \alpha + O(\alpha)^3 \\ \cos \alpha &= 1 + O(\alpha)^2\end{aligned}$$

we see that the first-order approximations to the input vector fields g_1 and g_2 are:

$$\tilde{g}_1 = \begin{pmatrix} 1 \\ \theta_0 \\ 0 \\ \theta_0 - \theta_1 \\ \theta_1 - \theta_2 \end{pmatrix} \quad \tilde{g}_2 = \begin{pmatrix} 0 \\ 0 \\ 1 \\ 0 \\ 0 \end{pmatrix}$$

These approximations are valid locally around $\theta_0 = 0, \theta_1 = 0, \theta_2 = 0$. Using the notation

$$\begin{aligned}\tilde{g}_3 &= [\tilde{g}_1, \tilde{g}_2] \\ \tilde{g}_4 &= [\tilde{g}_1, [\tilde{g}_1, \tilde{g}_2]] \\ \tilde{g}_5 &= [\tilde{g}_1, [\tilde{g}_1, [\tilde{g}_1, \tilde{g}_2]]]\end{aligned}$$

We find the distributions:

$$\tilde{\Delta}_0 = \text{span}\{\tilde{g}_1, \tilde{g}_2, \tilde{g}_3, \tilde{g}_4, \tilde{g}_5\}$$

$$\begin{aligned}
&= \text{span} \left\{ \begin{pmatrix} 1 \\ \theta_0 \\ 0 \\ \theta_0 - \theta_1 \\ \theta_1 - \theta_2 \end{pmatrix} \begin{pmatrix} 0 \\ 0 \\ 1 \\ 0 \\ 0 \end{pmatrix} \begin{pmatrix} 0 \\ -1 \\ 0 \\ -1 \\ 0 \end{pmatrix} \begin{pmatrix} 0 \\ 0 \\ 0 \\ -1 \\ 1 \end{pmatrix} \begin{pmatrix} 0 \\ 0 \\ 0 \\ -1 \\ 2 \end{pmatrix} \right\} \\
\tilde{\Delta}_1 &= \text{span}\{\tilde{g}_2, \tilde{g}_3, \tilde{g}_4\} \\
&= \text{span} \left\{ \begin{pmatrix} 0 \\ 0 \\ 1 \\ 0 \\ 0 \end{pmatrix} \begin{pmatrix} 0 \\ -1 \\ 0 \\ -1 \\ 0 \end{pmatrix} \begin{pmatrix} 0 \\ 0 \\ 0 \\ -1 \\ 1 \end{pmatrix} \right\}
\end{aligned}$$

We note that $\tilde{\Delta}_0$ has full rank and that $\tilde{\Delta}_1$ is involutive, since it is the span of constant vector fields. We now search for a function

$$\begin{aligned}
h : \mathbf{R}^2 \times S^1 \times S^1 \times S^1 &\longrightarrow \mathbf{R} \\
dh \cdot \tilde{\Delta}_1 &= 0 \tag{9}
\end{aligned}$$

$$dh \cdot \tilde{g}_5 \neq 0 \tag{10}$$

and we see that

$$h(x_0, y_0, \theta_0, \theta_1, \theta_2) = y_0 - \theta_1 - \theta_2$$

will satisfy the conditions (9) and (10).

We can now form the change of coordinates defined in the proposition as

$$\begin{aligned}
\xi_1 &= x_0 \\
\xi_2 &= L_{\tilde{g}_1}^3 h = \theta_0 - 2\theta_1 + \theta_2 \\
\xi_3 &= L_{\tilde{g}_1}^2 h = \theta_1 - \theta_2 \\
\xi_4 &= L_{\tilde{g}_1} h = \theta_2 \\
\xi_5 &= h = y - \theta_1 - \theta_2
\end{aligned}$$

and a state feedback of the form:

$$\begin{aligned}
v_1 &= u_1 \\
v_2 &= (L_{g_1} L_{\tilde{g}_1}^3 h)u_1 + (L_{g_2} L_{\tilde{g}_1}^3 h)u_2 \\
&= \frac{\cos(\theta_0 - \theta_1) \sin(\theta_1 - \theta_1) - 2 \sin(\theta_0 - \theta_1)}{\cos \theta_0} u_1 + u_2
\end{aligned}$$

will put the system into order- ρ chained form, $\rho = 1$.

In these coordinates, the differential equations look like:

$$\dot{\xi}_1 = v_1$$

$$\dot{\xi}_2 = v_2$$

$$\begin{aligned}\dot{\xi}_3 &= v_1 \frac{\sin(\xi_2 + \xi_3) - \cos(\xi_2 + \xi_3) \sin \xi_3}{\cos(\xi_2 + 2\xi_3 + \xi_4)} \\ \dot{\xi}_4 &= v_1 \frac{\cos(\xi_2 + \xi_3) \sin \xi_3}{\cos(\xi_2 + 2\xi_3 + \xi_4)} \\ \dot{\xi}_5 &= v_1 \frac{\sin(\xi_2 + 2\xi_3 + \xi_4) - \sin(\xi_2 + \xi_3) - \cos(\xi_2 + \xi_3) \sin \xi_3}{\cos(\xi_2 + 2\xi_3 + \xi_4)}\end{aligned}$$

which look quite complicated, but agree with the chained form to first order.

Because this is only an approximate chained form, the steering algorithm 1 cannot be used to steer this system. The usefulness of this particular coordinate transformation will be shown in Section 6

5 High-Frequency, High-Magnitude Sinusoids

Although the step-by-step sinusoids method presented in the previous section is an important result, it is limited because not all systems can be transformed into the required chained canonical form and because it makes no allowance for obstacle avoidance. In this chapter, we develop a method for steering nonholonomic systems which is universally applicable to any completely controllable drift-free system of the form

$$\dot{x} = \sum_{i=1}^m g_i(x) u_i \quad (11)$$

The results presented in this chapter were originally proposed by Sussmann and Liu [24, 25].

A sequence of inputs $\{u^j\}$ will be constructed, which generates a sequence of feasible trajectories $x^j(t)$. This sequence of trajectories will converge to a nominal trajectory $\gamma(t)$ in a sense to be made precise in this section. This nominal path $\gamma(t)$ can be any differentiable trajectory through the state space Q , *i.e.* $\gamma(t) \in C^1([0, T], Q)$. If desired, $\gamma(t)$ can be chosen to avoid any obstacles that may be present. In most cases, $\gamma(t)$ will not be a feasible path, meaning that it will not satisfy the nonholonomic constraints. We will see how it can be “approximated” with feasible trajectories.

The method described by Sussmann and Liu in [25] is quite complicated in its general form, and so in this paper we will present only those results which apply to the particular example we have chosen, the system consisting of a car-like mobile robot with two trailers. The system equations once again are:

$$\dot{x} = g_1(x) u_1 + g_2(x) u_2$$

where the state $x = (x_0, y_0, \theta_0, \theta_1, \theta_2)^T$ and the input vector fields g_1 and g_2 are

$$g_1 = \begin{pmatrix} \cos \theta_0 \\ \sin \theta_0 \\ 0 \\ \sin(\theta_0 - \theta_1) \\ \cos(\theta_0 - \theta_1) \sin(\theta_1 - \theta_2) \end{pmatrix} \quad g_2 = \begin{pmatrix} 0 \\ 0 \\ 1 \\ 0 \\ 0 \end{pmatrix}$$

5.1 P. Hall Basis

In order to present the results of Sussmann and Liu, we will need the definition of a P. Hall basis [5], a basis for the Lie algebra generated by a set of vector fields. Because Lie brackets satisfy

skew-symmetry and the Jacobi identity, there are certain dependencies among them, for example

$$\begin{aligned} [g_i, g_j] &= -[g_j, g_i] \\ [g_i, [g_j, g_k]] &= -[g_j, [g_k, g_i]] - [g_k, [g_i, g_j]] \end{aligned}$$

A basis for the set of all Lie brackets of $\{g_1, \dots, g_m\}$ must not include these linearly dependent elements.

We will need the notion of the *degree* of a Lie bracket $B = [B_1, B_2]$, which is defined as the sum of the degrees of its components, $\delta(B) = \delta(B_1) + \delta(B_2)$. If B is one of the generators of the Lie algebra, then $\delta(B) = 1$. For our example system, the generators are $\{g_1, g_2\}$ and we see

$$\begin{aligned} \delta(g_1) = \delta(g_2) &= 1 \\ \delta([g_1, g_2]) &= 2 \\ \delta([g_1, [g_1, g_2]]) &= 3 \\ \delta([g_2, [g_1, g_2]]) &= 3 \\ \delta([g_1, [g_1, [g_1, g_2]]]) &= 4 \\ &\vdots \end{aligned}$$

We let \mathcal{B} represent the set of all P. Hall basis elements. \mathcal{B} can be ordered by a relation $<$, and satisfies the following properties (for the two-generator case):

- (PH1) $g_1 < g_2 \in \mathcal{B}$
- (PH2) If $B_1, B_2 \in \mathcal{B}$ and $\delta(B_1) < \delta(B_2)$, then $B_1 < B_2$
- (PH3) $B = [B_1, B_2] \in \mathcal{B}$ if and only if
 - (a) $B_1, B_2 \in \mathcal{B}$, $B_1 < B_2$ and
 - (b) $B_2 = g_1$ or g_2 or $[B_3, B_4]$ where $B_3 \leq B_1$

For the two-trailer system we are using for our example, we arbitrarily choose $g_1 < g_2$. The elements of the P. Hall basis up to degree 4 are thus

$$\begin{aligned} &g_1 \\ &g_2 \\ &g_{1,2} = [g_1, g_2] =: g_3 \\ &g_{1,1,2} = [g_1, [g_1, g_2]] =: g_4 \\ &g_{1,1,1,2} = [g_1, [g_1, [g_1, g_2]]] =: g_5 \\ &g_{2,1,2} = [g_2, [g_1, g_2]] =: g_6 \\ &g_{2,1,1,2} = [g_2, [g_1, [g_1, g_2]]] =: g_7 \\ &g_{2,2,1,2} = [g_2, [g_2, [g_1, g_2]]] =: g_8 \end{aligned} \tag{12}$$

Note that we have assigned labels $\{g_3, \dots, g_8\}$ to these basis elements to avoid using the long indices that characterize each bracket, and that these labels do not correspond to the ordering of the P. Hall Basis. We have chosen this seemingly arbitrary ordering because for our example system of the mobile robot with two trailers, the brackets $\{g_1, g_2, g_3, g_4, g_5\}$ are linearly independent and therefore span the tangent space to the configuration space except where $\theta_0 - \theta_1 = \frac{\pi}{2}$. We will be using these 5 vector fields quite frequently in the sequel.

We now define the vector fields \hat{B} ; their purpose will become clear in Section 5.2. These vector fields are obtained by reversing the indices of the brackets in the P. Hall basis. For example, if $B = [g_1, [g_1, g_2]]$ then $\hat{B} = [[g_2, g_1], g_1]$. The skew-symmetry properties of the Lie bracket imply that $\hat{B} = \pm B$. In fact,

$$\hat{B} = B(-1)^{\delta(B)-1} \quad (13)$$

Using the same numbering scheme introduced in equation (12), the vector fields \hat{g} in the P. Hall basis previously described are:

$$\begin{aligned} \hat{g}_1 &= g_1 \\ \hat{g}_2 &= g_2 \\ \hat{g}_3 &= [g_2, g_1] = -g_3 \\ \hat{g}_4 &= [[g_2, g_1], g_1] = g_4 \\ \hat{g}_5 &= [[[g_2, g_1], g_1], g_1] = -g_5 \\ \hat{g}_6 &= [[g_2, g_1], g_2] = g_6 \\ \hat{g}_7 &= [[[g_2, g_1], g_1], g_2] = -g_7 \\ \hat{g}_8 &= [[[[g_2, g_1], g_2], g_2] = -g_8 \end{aligned}$$

5.2 The Chen-Fliess Expansion

If the control inputs $\{u_i(t)\}$ to a system are known, then the P. Hall basis can be used to write the Chen-Fliess functional expansion of the system. The Chen-Fliess expansion is an infinite series with one term for each bracket $B \in \mathcal{B}$, and coefficient functions which are iterated integrals of the inputs. It is useful to work with the system in this form, since the convergence properties of the inputs and trajectories can be easily seen. In this paper we will only state the main convergence result; the reader is encouraged to consult [23] for more detail on the Chen-Fliess expansion, and [25] for the proofs of the convergence results that are stated here.

Consider a drift-free control system of the form

$$\dot{x} = \sum_{i=1}^m g_i(x) u_i \quad (14)$$

and a sequence of inputs $\{u_i\}^j$ defined on the time interval $[0, T]$. It can be shown that the sequence of trajectories

$$\dot{x}^j = \sum_{i=1}^m g_i(x) u_i^j \quad (15)$$

will converge, under appropriate assumptions, to the solution of the Chen-Fliess functional expansion,

$$\dot{x}^\infty = \sum_{B \in \mathcal{B}} c_B^\infty(u)(t) \hat{B} \quad (16)$$

After we have defined the functions c_B^∞ used in equation (16), we will show how to construct an appropriate input sequence $\{u_i\}^j$ which will generate a given desired trajectory x^∞ .

As described in Section 5.1, \mathcal{B} is the P. Hall basis for the Lie algebra generated by the vector fields $\{g_1, \dots, g_m\}$, and the \hat{B} vector fields are related to the elements of the P. Hall basis as defined

in equation (13). With every bracket $B \in \mathcal{B}$ we will associate the two functions c_B and C_B , both of which depend on the input $u(t)$ and which are defined as follows.

If B is one of the generating vector fields ($B = g_i$), then we define c_B to be the corresponding input,

$$c_{g_i}(u)(t) = u_i(t), \quad 0 \leq t \leq T$$

We define C_B to be the integral of c_B ,

$$C_B(u)(t) = \int_0^t c_B(u)(\tau) d\tau \quad (17)$$

By definition, any bracket $B \neq g_i$ can be written as the Lie bracket of two other basis elements. However, instead of considering a simple Lie bracket, we find the largest k such that B can be written as

$$B = \text{ad}_{B_1}^k B_2 \quad (18)$$

where $B_1, B_2 \in \mathcal{B}$. We then define

$$c_B(u)(t) = \frac{1}{k!} [C_{B_1}(u)(t)]^k c_{B_2}(u)(t) \quad (19)$$

and C_B is once again the integral of c_B as in equation (17).

As mentioned earlier, we will be considering not just a single set of inputs $\{u_i\}$, but a sequence of these inputs $\{u_i\}^j$ indexed by the parameter j . We will define the functions $c_B^\infty(u)(t)$ as

$$c_B^\infty(u)(t) = \frac{d}{dt} \lim_{j \rightarrow \infty} C_B(u^j)(t) \quad (20)$$

Note that one does not simply take the limit of $c_B(u^j)(t)$ as $j \rightarrow \infty$, but that we must first integrate to get $C_B(u^j)(t)$, then take the limit, then differentiate. This is an important distinction.

The strategy for steering will be to find a sequence of inputs which generate a sequence of feasible trajectories, which, in the limit, converge to a motion in only one bracket direction. Because the system is completely controllable, the bracket directions will span the tangent space to the configuration space. The derivative of any desired trajectory $\gamma(t)$ is therefore in the span of the bracket directions,

$$\dot{\gamma}(t) = \sum_{B \in \mathcal{B}} b_B(t) B(\gamma(t))$$

We will show how a sequence of inputs that will generate motion in each one of these bracket directions B can be found, and then we simply sum these sequences together to get the total motion. If certain noninterference conditions among the frequencies present in the inputs hold, then the individual motions will also add due to a high-frequency superposition property that can be shown to hold for inputs of this form, see [25].

We therefore consider these bracket directions one at a time; let us start with the simplest bracket $[g_1, g_2]$. From our experiences with steering with sinusoids, we might postulate choosing an input of the form:

$$\begin{aligned} u_1(t) &= \alpha \sin \omega t \\ u_2(t) &= \beta \cos \omega t \end{aligned}$$

In fact the required input for asymptotic motion only in the $[g_1, g_2]$ direction is:

$$\begin{aligned} u_1^j(t) &= \eta_1(t)\sqrt{j} \sin(j\omega t) \\ u_2^j(t) &= \eta_2(t)\sqrt{j} \cos(j\omega t) \end{aligned} \quad (21)$$

and the magnitude of the asymptotic displacement is $\frac{1}{2\omega}\eta_1(t)\eta_2(t)$. This means that for any system of the form

$$\dot{x} = g_1(x)u_1 + g_2(x)u_2$$

with inputs as described in equation (21), the sequence of trajectories x^j will converge to the trajectory x^∞ satisfying:

$$\dot{x}^\infty = \frac{\eta_1(t)\eta_2(t)}{2\omega}[g_1, g_2](x)$$

To clarify some of the convergence results, we present the calculations for the relatively simple case when η_1, η_2 are constant functions of time. Similar results are obtained when these are time-varying (and analytic) using integration by parts, see [25].

The first two coefficient functions are simply the inputs,

$$\begin{aligned} c_{g_1}(t) &= u_1(t) = \eta_1\sqrt{j} \sin(j\omega t) \\ c_{g_2}(t) &= u_2(t) = \eta_2\sqrt{j} \cos(j\omega t) \end{aligned}$$

To find C_{g_1} and C_{g_2} we integrate,

$$\begin{aligned} C_{g_1}(t) &= \int_0^t c_{g_1}(\tau) d\tau \\ &= \frac{-\eta_1}{\omega\sqrt{j}} \cos(j\omega t) \xrightarrow{j \rightarrow \infty} 0 \\ C_{g_2}(t) &= \int_0^t c_{g_2}(\tau) d\tau \\ &= \frac{\eta_2}{\omega\sqrt{j}} \sin(j\omega t) \xrightarrow{j \rightarrow \infty} 0 \end{aligned}$$

and note that as $j \rightarrow \infty$, these two functions will converge uniformly to zero. Now, $g_3 = [g_1, g_2] = \text{ad}_{g_1}g_2$, and using Equation 19 as well as the functions just calculated, we can see that the coefficient functions associated with g_3 are:

$$\begin{aligned} c_{g_3}(t) &= C_{g_1}(t) \cdot c_{g_2}(t) \\ &= \frac{-\eta_1\eta_2}{\omega} \cos^2(j\omega t) \\ &= \frac{-\eta_1\eta_2}{\omega} \left[\frac{1}{2} + \frac{1}{2} \cos(2j\omega t) \right] \\ C_{g_3}(t) &= \int_0^t c_{g_3}(\tau) d\tau \\ &= \frac{-\eta_1\eta_2}{\omega} \left[\frac{1}{2}t + \frac{1}{4j\omega} \sin(2j\omega t) \right] \xrightarrow{j \rightarrow \infty} -\frac{\eta_1\eta_2}{2\omega}t \end{aligned}$$

We note that the function C_{g_3} is nonzero.

We can write g_4 as $[g_1, [g_1, g_2]] = \text{ad}_{g_1}^2 g_2$, and therefore

$$\begin{aligned} c_{g_4}(t) &= \frac{1}{2!} (C_{g_1}(t))^2 \cdot c_{g_2}(t) \\ &= \frac{\eta_1^2 \eta_2}{2\omega^2 \sqrt{j}} \cos^3(j\omega t) \\ C_{g_4}(t) &= \frac{\eta_1^2 \eta_2}{2\omega^3 j^{\frac{3}{2}}} [\sin(j\omega t) - \frac{1}{3} \sin^3(j\omega t)] \xrightarrow{j \rightarrow \infty} 0 \end{aligned}$$

Likewise, $C_{g_5}, \dots, C_{g_8} \xrightarrow{j \rightarrow \infty} 0$ uniformly on $[0, T]$. Indeed, because of the fact that each input is multiplied by $j^{\frac{1}{2}}$, all functions C_B associated with brackets B with degree $\delta(B) \neq 2$, will converge to zero in the limit.

Using equation (20), we can see that with input sequences u_1^j, u_2^j as in equation (21),

$$\begin{aligned} c_{g_3}^\infty &= -\frac{\eta_1 \eta_2}{2\omega} \\ c_B^\infty &= 0, \quad B \neq g_3 \end{aligned}$$

From equation (16), it can be seen that the Chen-Fliess expansion in the limit looks like:

$$\dot{x}^\infty = c_{g_3}^\infty \hat{g}_3(x)$$

and therefore, in the limit as $j \rightarrow \infty$, we will only get motion in the direction of the bracket $\hat{g}_3 = [g_2, g_1]$.

This result can be extended to other brackets by noticing that if the inputs are all sums of sinusoids with frequencies multiplied by j and magnitudes multiplied by $j^{\frac{k}{k+1}}$, that is

$$u_i^j(t) = j^{\frac{k}{k+1}} \sum_p \eta_{i,p}(t) \sin(j\omega_{i,p}t) + j^{\frac{k}{k+1}} \sum_q \eta_{i,q}(t) \cos(j\omega_{i,q}t)$$

then $C_B \xrightarrow{j \rightarrow \infty} 0$ for all B such that $\delta(B) \neq k+1$. We will want to intelligently choose the frequencies ω_p and ω_q so that exactly one of these functions C_B is nonzero.

If we again tried to draw a parallel with the step-by-step sinusoids method from Section 3, we might predict that if there were only one frequency in each input, and $\omega_2 = k\omega_1$, the function C_B would be nonzero for $B = \text{ad}_{g_1}^k g_2$ and zero for all other brackets B . This conjecture turns out to be true; in fact, after multiplying, integrating, and taking the limits, it can be seen that for inputs of the form:

$$\begin{aligned} u_1^j(t) &= \eta_1(t) j^{\frac{k}{k+1}} \sin(j\omega t) \\ u_2^j(t) &= \eta_2(t) j^{\frac{k}{k+1}} \cos(jk\omega t) \end{aligned}$$

the Chen-Fliess coefficient functions are

$$\begin{aligned} c_B^\infty &= \frac{(-1)^k \eta_1^k \eta_2}{k! (2\omega)^k}, \quad B = \text{ad}_{g_1}^k g_2 \\ c_B^\infty &= 0, \quad B \neq \text{ad}_{g_1}^k g_2 \end{aligned}$$

These coefficients are the same as those in the chained-form, step-by-step sinusoids result from Algorithm 1.

5.3 Choosing the Control Inputs

From the derivations in the previous section, it can be seen that inputs which take the general form of sums of sinusoids will result in many of the Chen-Fliess coefficients asymptotically going to zero, and the remaining coefficients having a simple, closed form. Here we present a methodology for choosing the specific sequence of input functions, $\{u_i(t)\}^j$, which will generate a sequence of trajectories $x^j(t)$ converging to a desired trajectory $\gamma(t)$. While doing this in detail for the two-trailer system, we will also show some of the general theory.

Once again, we start with a controllable drift-free control system of the form

$$\dot{x} = \sum_{i=1}^m g_i(x)u_i$$

and let \mathcal{B} represent the P. Hall basis for the Lie algebra generated by the input vector fields $\{g_1, \dots, g_m\}$. Consider all elements of \mathcal{B} whose degree is less than or equal to some number d . This number d is chosen to be large enough so that

$$\text{span}\{B \in \mathcal{B} \mid \delta(B) \leq d\} = T_x Q \quad \forall x \in U$$

i.e. these brackets span the tangent space to the state space Q at every point in some open set U of interest. For convenience, we will label those brackets which have degree less than or equal to d as $\{g_1, \dots, g_m, \dots, g_r\}$; the first m of these being the input vector fields g_i . Note that necessarily $r \geq n = \dim Q$.

Now consider an “extended system” formulated on Q as

$$\dot{x} = \sum_{i=1}^r \hat{g}_i(x)v_i$$

where we have again used the notation $\hat{g} = (-1)^{\delta(g)-1}g$. This system is also completely controllable; by definition

$$\text{span}\{g_1, \dots, g_m, \dots, g_r\} = TQ$$

Given any desired trajectory $\gamma(t)$, the system of equations

$$\dot{\gamma}(t) = \sum_{i=1}^r \hat{g}_i(\gamma(t))v_i(t) \tag{22}$$

can be solved for the functions $v_i(t)$ using an inverse or pseudo-inverse method. The functions (v_1, \dots, v_r) are called the *extended inputs*. If $r > n$ then there may be many different extended inputs which will generate the same trajectory $\gamma(t)$.

The sequence of real inputs $\{u_i\}^j$ will be chosen so that the Chen-Fliess expansion has the desired coefficients. Recall that in the limit, the expansion will have the form

$$\begin{aligned} \dot{x}^\infty &= \sum_{B \in \mathcal{B}} c_B^\infty(u)(t)\hat{B} \\ &= \sum_{i=1}^r c_{g_i}^\infty(u)(t)\hat{g}_i + \sum_{\substack{B \in \mathcal{B} \\ \delta(B) > d}} c_B^\infty(u)(t)\hat{B} \end{aligned} \tag{23}$$

and so by comparing equations (23) and (22), it can be seen from setting $x^\infty = \gamma$, that the sequence of inputs should be chosen so that the Chen-Fliess coefficients c_B are related to the extended inputs by:

$$\begin{aligned} c_{g_i}^\infty(u)(t) &= v_i(t), & i &= 1, \dots, r \\ c_B^\infty(u)(t) &= 0, & \delta(B) &> d \end{aligned} \quad (24)$$

It can be verified that inputs which are sums of sinusoids of the following form will suffice:

$$u_i^j = \sum_p \eta_{i,p}(t) j^{\frac{k_p}{k_p+1}} \sin(j\omega_{i,p}t) + \sum_q \eta_{i,q}(t) j^{\frac{k_q}{k_q+1}} \cos(j\omega_{i,q}t)$$

Of course some care must be taken when choosing the frequencies $\omega_{i,p}, \omega_{i,q}$ and the coefficient functions $\eta_{i,p}(t), \eta_{i,q}(t)$ so that the Chen-Fliess coefficient functions c_B^∞ will be as defined in equation (24).

Returning to the two-trailer problem, it was shown in Section 2 that the set of brackets

$$\{g_1, g_2, [g_1, g_2], [g_1, [g_1, g_2]], [g_1, [g_1, [g_1, g_2]]]\}$$

will span the tangent space on the open set $U = \{(x_0, y_0, \theta_0, \theta_1, \theta_2) : \theta_0 - \theta_1 \neq \pm \frac{\pi}{2}\}$. The maximum degree of these brackets is 4; therefore we consider all elements of the P. Hall basis with degree less than or equal to 4. In Section 5.1 it was shown that there are 8 of these brackets, $\{g_1, \dots, g_8\}$; they were enumerated in equation (12). Now, given any desired trajectory $\gamma(t)$, we first need to find the extended inputs $\{v_i\}$ which satisfy the equation

$$\dot{\gamma}(t) = \sum_{i=1}^8 \hat{g}_i(\gamma(t)) v_i(t)$$

Since $8 > 5 = \dim Q$, there will be many such extended inputs. However, since the set $\{g_1, \dots, g_5\}$ will suffice to span, we can choose $v_6 = v_7 = v_8 \equiv 0$, and be left with 5 equations and 5 unknowns. We then solve uniquely for (v_1, \dots, v_5) :

$$\begin{aligned} \begin{bmatrix} v_1(t) \\ \vdots \\ v_5(t) \end{bmatrix} &= \begin{bmatrix} | & & | \\ g_1(\gamma(t)) & \cdots & g_5(\gamma(t)) \\ | & & | \end{bmatrix}^{-1} \begin{bmatrix} | \\ \dot{\gamma}(t) \\ | \end{bmatrix} \\ v(t) &= \tilde{G}(\gamma)^{-1} \dot{\gamma}(t) \end{aligned} \quad (25)$$

It should be noted that the matrix $\tilde{G}(\gamma)$ will be nonsingular for all paths $\gamma(t) \in U$.

The sequence of inputs which will result in the desired convergence properties has the form

$$\begin{aligned} u_1^j &= \eta_{1,0} + j^{1/2} \eta_{1,1} \sin(j\omega_1 t) + j^{2/3} \eta_{1,2} \sin(j\omega_2 t) + j^{3/4} \eta_{1,3} \sin(j\omega_3 t) \\ u_2^j &= \eta_{2,0} + j^{1/2} \eta_{2,1} \cos(j\omega_1 t) + j^{2/3} \eta_{2,2} \cos(j\omega_2 t) + j^{3/4} \eta_{2,3} \cos(j\omega_3 t) \end{aligned} \quad (26)$$

and provided that certain noninterference conditions between $\omega_1, \omega_2, \omega_3$ are satisfied, the corresponding Chen-Fliess coefficient functions are

$$c_{g_1} = \eta_{1,0} \quad (27)$$

$$c_{g_2} = \eta_{2,0} \quad (28)$$

$$c_{g_3} = -\frac{\eta_{1,1}\eta_{2,1}}{2\omega_1} \quad (29)$$

$$c_{g_4} = \frac{\eta_{1,2}^2\eta_{2,2}}{8\omega_2^2} \quad (30)$$

$$c_{g_5} = -\frac{\eta_{1,3}^3\eta_{2,3}}{48\omega_3^3} \quad (31)$$

$$c_{g_i} = 0, \quad i > 5$$

Therefore, once the frequencies $\{\omega_1, \omega_2, \omega_3\}$ have been chosen to satisfy the noninterference conditions (described in the following section), the functions $\eta_{i,k}$ can be chosen so that the Chen-Fliess coefficients given by equations (27)–(31) are equal to the extended inputs (25), or

$$\begin{aligned} \eta_{1,0}(t) &= v_1(t) \\ \eta_{2,0}(t) &= v_2(t) \\ \eta_{1,1}(t)\eta_{2,1}(t) &= -2\omega_1 v_3(t) \\ \eta_{1,2}^2(t)\eta_{2,2}(t) &= 8\omega_2^2 v_4(t) \\ \eta_{1,3}^3(t)\eta_{2,3}(t) &= -48\omega_3^3 v_5(t) \end{aligned}$$

Note that even though the extended input $\{v_1(t), \dots, v_5(t)\}$ is unique, there is still some freedom in the choice of the functions $\eta_{i,k}$.

5.4 Noninterference Conditions

In Sussmann and Liu's paper, the noninterference conditions are formulated as independence relations among various sets. Since the notation becomes cumbersome for the general case, we will only describe the noninterference conditions for the example system. Of course these will be the same as for any 5-state, 2-input system with

$$\{g_1, g_2, [g_1, g_2], [g_1, [g_1, g_2]], [g_1, [g_1, [g_1, g_2]]]\}$$

linearly independent. These conditions are derived from the Chen-Fliess coefficients.

Consider the inputs of equation (26), repeated here for convenience:

$$\begin{aligned} u_1^j &= \eta_{1,0} + j^{1/2}\eta_{1,1} \sin(j\omega_1 t) + j^{2/3}\eta_{1,2} \sin(j\omega_2 t) + j^{3/4}\eta_{1,3} \sin(j\omega_3 t) \\ u_2^j &= \eta_{2,0} + j^{1/2}\eta_{2,1} \cos(j\omega_1 t) + j^{2/3}\eta_{2,2} \cos(j\omega_2 t) + j^{3/4}\eta_{2,3} \cos(j\omega_3 t) \end{aligned}$$

and define the two sets Ω_1, Ω_2 to be:

$$\begin{aligned} \Omega_1 &= \{\pm\omega_1, \pm\omega_2, \pm\omega_3, \pm\omega_4\} \\ \Omega_2 &= \{\pm\omega_1, \pm 2\omega_2, \pm 3\omega_3, \pm 4\omega_4\} \end{aligned} \quad (32)$$

Ω_i is the set of all frequencies contained in the input u_i .

For any bracket $B \in \mathcal{B}$, we can define its first degree δ_1 and its second degree δ_2 . These degrees correspond to the number of times the generating vector fields g_1 and g_2 respectively appear in the

expression of the bracket. For example, if $B = [g_1, [g_1, g_2]]$ then $\delta_1(B) = 2$ and $\delta_2(B) = 1$. It is easily seen that for every bracket B ,

$$\delta(B) = \delta_1(B) + \delta_2(B)$$

In order to generate motion in a bracket direction B with $\delta_1(B) = d_1$ and $\delta_2(B) = d_2$, the sum of d_1 of the frequencies in Ω_1 with d_2 of the frequencies in Ω_2 must equal zero, that is

$$\sum_{p=1}^{d_1} \nu_p + \sum_{q=1}^{d_2} \zeta_q = 0 \quad (33)$$

with $\nu_p \in \Omega_1$ and $\zeta_q \in \Omega_2$. However, to prevent interference, there should be *exactly one* such combination $\{\nu_1, \dots, \nu_{d_1}, \zeta_1, \dots, \zeta_{d_2}\}$ ⁵.

For all bracket directions $B \in \mathcal{B}$ in which motion is not desired, there should be *no* combinations $\nu_p \in \Omega_1$ and $\zeta_q \in \Omega_2$ such that

$$\sum_{p=1}^{\delta_1(B)} \nu_p + \sum_{q=1}^{\delta_2(B)} \zeta_q = 0$$

Consider, by way of example, the bracket $B = [g_1, [g_1, g_2]]$, $\delta_1(B) = 2$, $\delta_2(B) = 1$. It can be seen that for the frequencies given in equation (32), the equation

$$\nu_1 + \nu_2 + \zeta_1 = 0 \quad (34)$$

is satisfied for $\nu_1 = \nu_2 = \omega_2$, and $\zeta_1 = -2\omega_2$. However, it must be verified that this is the *only* such combination satisfying equation (34).

The bracket $B = [g_2, [g_1, g_2]]$, $\delta_1(B) = 1$, $\delta_2(B) = 2$ is a direction in which we do not wish to move. Therefore, it must be checked that there do not exist frequencies $\nu_1 \in \Omega_1, \zeta_1, \zeta_2 \in \Omega_2$ such that

$$\nu_1 + \zeta_1 + \zeta_2 = 0$$

If one takes the trouble to calculate all the coefficient functions c_B^∞ for the inputs $\{u_i\}^j$ as given, it is easy to see how the noninterference conditions are derived from relations among the various frequencies involved. For the coefficient corresponding to a bracket with $\delta_1(B) = d_1$ and $\delta_2(B) = d_2$, it can be seen that there will be d_1 copies of the function u_1 and d_2 copies of the function u_2 in the expression for $c_B(u)(t)$. The inputs u_1 and u_2 are sums of sinusoids; when they are multiplied, new frequencies appear, corresponding to the sums and differences of the original frequencies. The frequencies present in c_B therefore will be all possible combinations of d_1 of the frequencies from the set Ω_1 and d_2 of the frequencies from Ω_2 . Recalling that all of the frequencies are multiplied by the parameter j , we see that if none of these combinations sum to zero, all the terms will be divided by j when c_B is integrated to find C_B , and thus these terms will all go to zero in the limit when c_B^∞ is calculated. If, however, there is a zero-frequency term, it will not be divided by j when c_B is integrated to get C_B , in which case c_B^∞ will be non-zero. It is an instructive exercise to perform these integrations and realize how the inputs are interacting to give the desired motions.

⁵excepting, of course, the combination $\{-\nu_1, \dots, -\nu_{d_1}, -\zeta_1, \dots, -\zeta_{d_2}\}$ which will also satisfy equation (33).

5.5 Connections to Step-by-step Sinusoids

It is interesting to note the similarities between the extended input above and the corresponding functions in the Murray and Sastry algorithm presented in Section 3. If we formulate the 5-dimensional chained system as:

$$\begin{aligned} g_1 &= (1, 0, x_1, x_2, x_3)^T \\ g_2 &= (0, 1, 0, 0, 0)^T \\ g_3 &= (0, 0, 1, 0, 0)^T = \text{ad}_{g_1} g_2 \\ g_4 &= (0, 0, 0, 1, 0)^T = \text{ad}_{g_1}^2 g_2 \\ g_5 &= (0, 0, 0, 0, 1)^T = \text{ad}_{g_1}^3 g_2 \end{aligned}$$

then we would use the following inputs to get motion in each direction:

$$\begin{aligned} u_1 &= \alpha & \Delta x_1 &= \alpha T \\ u_2 &= \beta & \Delta x_2 &= \beta T \\ \begin{cases} u_1 = \alpha \sin \omega t \\ u_2 = \beta \cos \omega t \end{cases} & & \Delta x_3 &= \frac{\alpha \beta}{2\omega} T \\ \begin{cases} u_1 = \alpha \sin \omega t \\ u_2 = \beta \cos 2\omega t \end{cases} & & \Delta x_4 &= \frac{\alpha^2 \beta}{8\omega^2} T \\ \begin{cases} u_1 = \alpha \sin \omega t \\ u_2 = \beta \cos 3\omega t \end{cases} & & \Delta x_5 &= \frac{\alpha^3 \beta}{48\omega^3} T \end{aligned}$$

Compare these with the extended inputs described by equations (27)-(31), which are

$$\begin{aligned} c_{g_1} &= \eta_{1,0} \\ c_{g_2} &= \eta_{2,0} \\ c_{g_3} &= -\frac{\eta_{1,1}\eta_{2,1}}{2\omega_1} \\ c_{g_4} &= \frac{\eta_{1,2}^2\eta_{2,2}}{8\omega_2^2} \\ c_{g_5} &= -\frac{\eta_{1,3}^3\eta_{2,3}}{48\omega_3^3} \end{aligned}$$

Because of the special forms of the bracket directions in the chained system, Δx_i is the same as motion in the direction of the vector field g_i . The differences in the minus signs result from the definitions of the vector fields \hat{g}_i , and the factor of T is subsumed in the extended input v .

What is especially striking is that although Murray and Sastry's result was only shown to work for systems in chained form, the result we have stated is for *any* system in the form (11) such that the brackets $\{g_1, g_2, \text{ad}_{g_1} g_2, \text{ad}_{g_1}^2 g_2, \text{ad}_{g_1}^3 g_2\}$ are linearly independent. The Murray and Sastry result effectively used $j = 1$, whereas this scheme works in the limit as $j \rightarrow \infty$.

5.6 Summary of High-Frequency, High-Magnitude Sinusoids

Here we should note that we have not presented Sussmann and Liu's algorithm exactly, but rather used their idea of high frequency, high amplitude inputs and letting the parameter $j \rightarrow \infty$ to

eliminate the interference caused by trying to steer using sinusoids all at once. We have used only two frequencies for each bracket direction; their algorithm uses n frequencies to generate motion in the direction of a degree n Lie Bracket. Although it is not clear that a simplification such as ours would work for every case, it does work for the systems discussed here, and indeed for any system spanned by vector fields of the form $\{\text{ad}_{g_1}^k g_2\}$. Their complete theory is quite general and complex and cannot be completely examined here. For a much more exhaustive treatment, see [25].

One of the main advantages of the high-frequency sinusoids method presented in this section is that the desired path can be chosen in advance, perhaps from a solution to the holonomic obstacle-avoidance problem. Ideally, once the obstacle-free path is found, the parameter j in the inputs could be chosen to be large enough so that the resulting feasible path is clear of obstacles.

However, it can be seen that when j increases, and the desired path is more closely followed, the frequency and magnitude of the inputs increase. These inputs may not be realistic. Also, the resulting paths are highly oscillatory, and the rate of convergence depends on the chosen path as well as the choice of coordinates.

6 Applications and Simulations

In this section, we present some simulation results for the high-frequency sinusoids method of Sussmann and Liu which was presented in the previous section. All of the simulations were done using the program `Simulate.m`, a numerical integration routine in the Mathematica programming environment. We have run simulations for two desired trajectories, using two different sets of coordinates, and for various values of the parameter j to see how the convergence is realized in a practical system.

6.1 The Parallel-Parking Trajectory

The first trajectory that we chose to simulate corresponds to a parallel-parking maneuver, moving the lead car and both trailers sideways. We start with the trailers lined up directly behind the lead car, $x^o = (0, 1, 0, 0, 0)$ and try to move the entire system to a final position $x^f = (0, 0, 0, 0, 0)$, also with the trailers aligned. See Figure 2 for the chosen trajectory.

To satisfy the non-interference conditions, we chose the frequencies $\omega_1 = \frac{5}{8}$, $\omega_2 = \frac{6}{7}$, and $\omega_3 = 1$. These were chosen by checking the conditions of Section 5.4 for these frequencies and all brackets B with degree less than 4.

When we were choosing our desired trajectory, we wanted to be sure that we avoided the point of singularity, $\theta_1 = \theta_0 \pm \frac{\pi}{2}$. Therefore, to keep our inputs small enough, and the trajectory far away from this point, we chose a linear parameterization of the straight path from x^o to x^f along 100 seconds. We also scaled all the frequencies by $\frac{2\pi}{10}$. Note that this straight-line path is not feasible for the system.

We simulated the system in both the original coordinates and in the order-1 chained form coordinates. We expected that the convergence properties would be improved by using the approximate chained form, since the bracket directions that we are not trying to move in consist of only higher order terms. The results that we have obtained confirm that hypothesis.

It can be seen that for both sets of coordinates, the desired path is more closely followed as j goes from 1 to 100. The improved tracking for the transformed coordinates is remarkable. The position error for the transformed coordinates at $j = 1$ is less than the error for the standard

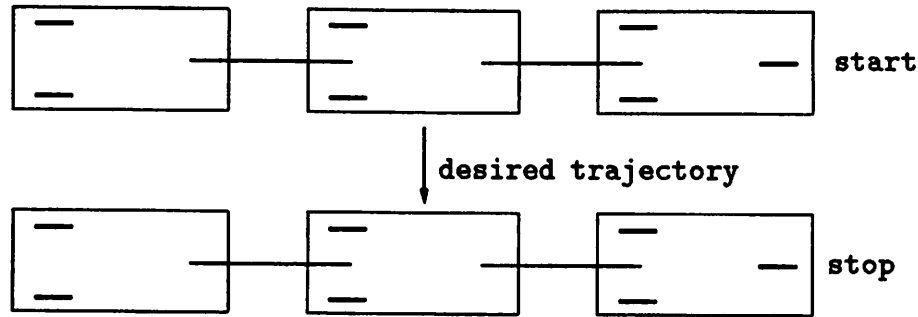


Figure 2: The Chosen Parallel-Parking Trajectory.

coordinates at $j = 10$. We have gained more than a factor of 10 in the frequencies needed to achieve a given trajectory error merely by changing coordinates. There could conceivably exist another set of coordinates in which the convergence would be even faster; however, it is not clear how to go about searching for such a coordinate transformation.

In order to show the highly oscillatory nature of these paths, we have included one plot showing the trajectories of all five states, see Figure 5. The desired trajectory is:

$$\begin{aligned}
 x(t) &\equiv 0 \\
 y(t) &= 1 - \frac{t}{100} \\
 \theta_0(t) &\equiv 0 \\
 \theta_1(t) &\equiv 0 \\
 \theta_2(t) &\equiv 0
 \end{aligned}$$

It can be seen that the actual trajectory stays near this path, but diverges from it many times.

It should be noted that one of the reasons that the transformed coordinates worked particularly well along the parallel-parking trajectory was that the higher order terms were all very small along the chosen path ($\theta_0 = \theta_1 = \theta_2 = 0$). From initial simulation results with other paths, these coordinates do not seem to improve the behavior of the convergence in general. However, it is important to note how much the error can depend on the choice of coordinates.

6.2 The Corner Trajectory

In order to see how the steering algorithm worked on a perhaps more realistic trajectory, we decided to have the car-like robot with trailers follow a path around a corner.

The desired trajectory was specified as driving straight for 50 seconds, then following the arc of a circle through 90 degrees taking another 50 seconds, then straightening out again for the final 50 seconds of the trajectory. The simulation results follow for $j = 10$ and $j = 100$.

It is perhaps insightful to look at the plot of the (x_0, y_0) variables, the position in the plane of the lead car, see Figure 6. In this figure, we have removed the scaling by time, and shown the actual path in the x - y plane that the lead car follows. The trajectories of the two trailers are similar.

Notice that there are three parts to the trajectory, but since this is an open-loop strategy we do not end up exactly where we hope to after the second segment (although in theory we could come as close as we wished by increasing the value of j) so that the third segment, which should be a

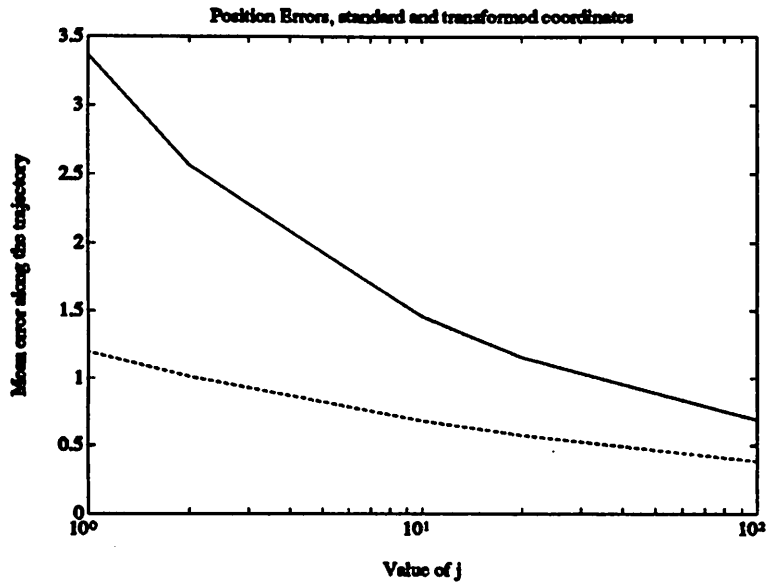


Figure 3: Position errors for various values of j , in standard (solid line) and transformed (dashed line) coordinates. The error is calculated as the root-mean-square distance from the straight-line parallel-parking trajectory.

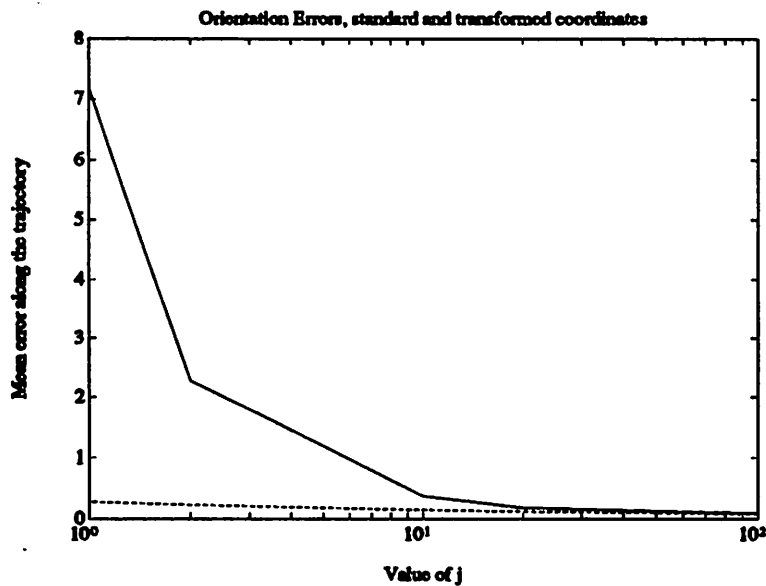


Figure 4: Orientation errors for various values of j , in standard (solid line) and transformed (dashed line) coordinates. The error is calculated as the root-mean-square distance (in radians) from the desired parallel-parking trajectory, in which all angles are identically zero.

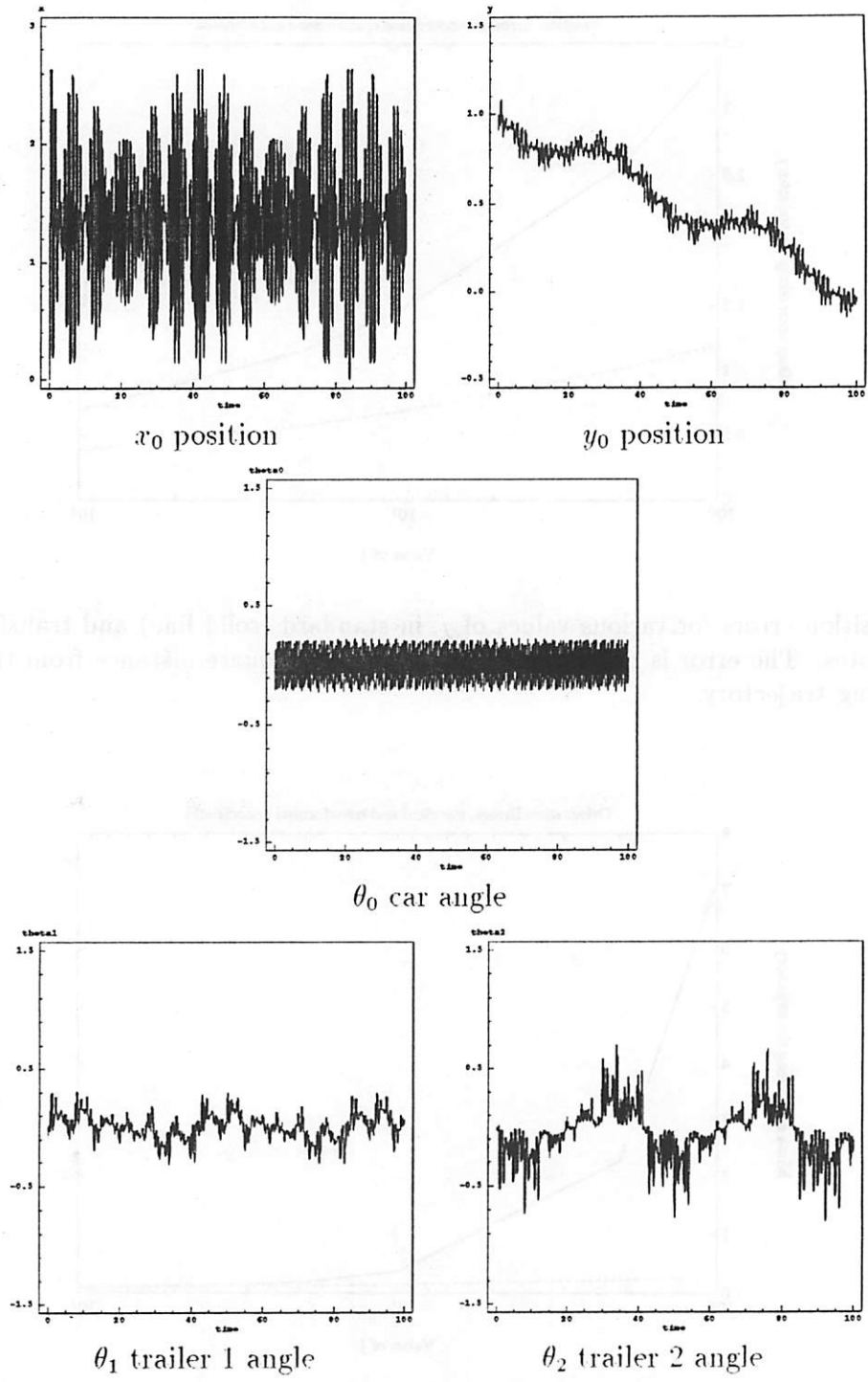


Figure 5: Steering the System in Standard Coordinates. $j = 10$. The desired trajectory is the straight line $(0.1 - \frac{t}{100}, 0, 0, 0)$. As j increases, the trajectory becomes closer to the desired straight line, but oscillates about it at a higher frequency.

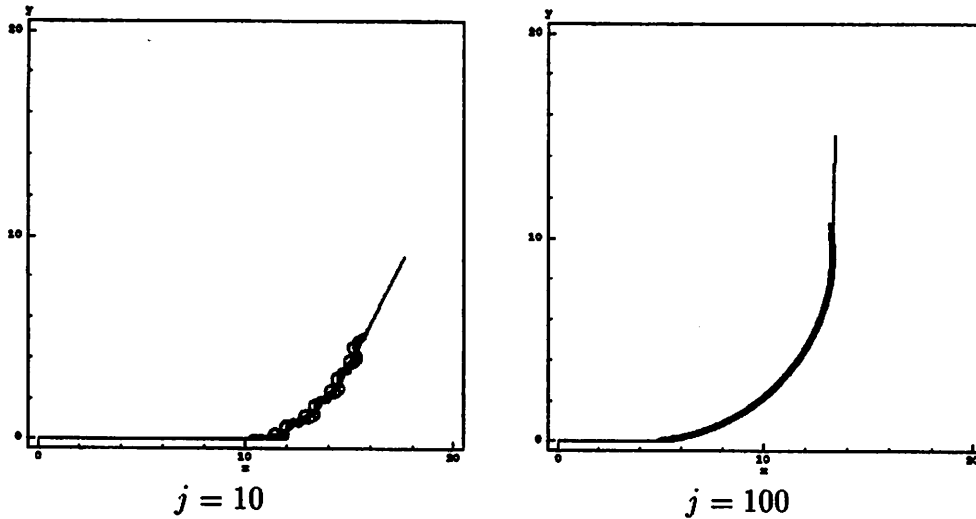


Figure 6: The (x_0, y_0) position of the lead car for two values of j , executing the corner turning trajectory

simple straight line, is in the wrong direction because of the initial error. This problem is inherent in any open-loop planning strategy.

It is interesting to note, that although the trailer angles are not at their desired positions after the second segment, they converge to zero during the third segment. This is a result of an attribute of this system of car-like robots with trailers which has not been fully exploited: symmetry and anti-symmetry. If the home configuration is chosen so that all the trailers are aligned ($\theta_1 = \theta_2 = \theta_0$), then for a positive driving input ($u_1 > 0$) this configuration is *stable* in the sense that if the trailer angles start off near zero they will approach zero as the lead car drives forward. However for $u_1 < 0$ (corresponding to the lead car backing up) this configuration is *unstable*; as the lead car backs up the trailer angles will grow away from zero.

To illustrate how impractical the high-frequency sinusoids method can seem, we tried a simple-minded approach to the problem of turning a corner using constant control inputs: drive straight for 50 seconds ($\{u_1, u_2\} = \{\frac{1}{10}, 0\}$), then turn the wheel while continuing to drive for the next 50 seconds, ($\{u_1, u_2\} = \{\frac{1}{10}, \frac{\pi}{100}\}$), then straighten out the steering wheel and drive straight again to finish off the path in the final 50 seconds ($\{u_1, u_2\} = \{\frac{1}{10}, 0\}$).

The resulting maneuver had the lead car following the desired circular arc trajectory exactly, but the orientations of the trailers lagged behind the orientation of the lead car. Since the desired trajectory had the trailers aligned with the lead car and this configuration is stable when the system is driving forwards, the trailer angles did converge to the desired values during the third part of the trajectory. The main difference between this approach and the high-frequency sinusoids is that in the simplistic approach we are only concerned about the position and orientation of the lead car; the trailers are just following behind. In the high-frequency sinusoids maneuver, we commanded the trailer angles to be the same as the car angle throughout the entire path $\theta_1 = \theta_2 = \theta_0$. It is by no means clear however that such a simplistic approach could be used for the reverse problem of backing up around a corner, or for the much more difficult problem of parallel-parking. For most paths, the high-frequency sinusoids method must be used.

7 Conclusions

In this paper, we presented and evaluated two different methods for steering car-like robots with trailers; both methods used combinations of sinusoidal functions as inputs. The step-by-step sinusoids method, presented in Section 3, was shown to work for systems in a special chained canonical form. A coordinate transformations to chained form was developed for the one-trailer system.

Since a conversion to chained form for the two-trailer system has not been found, an approximate chained form was proposed. This set of coordinates was shown to be useful in the second steering method.

The high-frequency sinusoids method, originally proposed by Sussmann and Liu [24], was presented in Section 5 in an abbreviated form. This method constructs a sequence of inputs $\{u_i\}^j$ which were sums of sinusoids of frequencies $j\omega_k$ with magnitudes $j^\alpha\eta_k$, where $0 < \alpha < 1$. As the parameter j goes to ∞ , the sequence of trajectories $\{x^j\}$ generated by the inputs $\{u_i\}^j$ converges uniformly to a desired infeasible path γ . This path γ can be chosen initially to avoid obstacles. However, as the trajectories $\{x^j\}$ become closer to this desired path γ , the inputs $\{u_i\}^j$ increase in both magnitude and frequency, making this an unreasonable method for steering a practical system.

Some sample paths that were generated by the high-frequency sinusoids method were seen in Section 6. As expected, the trajectories are highly oscillatory but do indeed converge to the desired path as predicted by the theory. The convergence rates were shown to be much improved for the approximate chained form coordinate system proposed herein. These results are significant in that they are the first time (to the authors' knowledge) that a control algorithm has been found for a car-like robot with two trailers.

The advantage of the high-frequency sinusoids method is that it is completely general and can be used for all systems and all trajectories. It does not seem to be a very practical method for use in real systems, because of the very high-magnitude, high-frequency inputs that are required and the highly oscillatory paths which result. If obstacles are present in the state space, however, this may be a good method to use since the obstacle-avoidance problem can be done in the much simpler holonomic framework, and this obstacle-free path can then be approximated arbitrarily closely.

Better algorithms could possibly be developed for this system by exploiting the inherent symmetry and anti-symmetry to advantage. It was shown in Section 6 that some trajectories can be approximated much more realistically using a simplistic approach that exploits the stability properties of certain trailer configurations. However, the number of such trajectories is very small. Methods such as the two presented in this paper can be used as general path planners for mobile robot systems with trailers, and indeed, any nonholonomic systems.

References

- [1] A. Bellaïche, J-P. Laumond, and P. Jacobs. Controllability of car-like robots and complexity of the motion planning problem with non-holonomic constraints. In *International Symposium on Intelligent control*, pages 322–337, Bangalore, India, 1991.
- [2] R. W. Brockett. Control theory and singular Riemannian geometry. In *New Directions in Applied Mathematics*, pages 11–27. Springer-Verlag, New York, 1981.

- [3] R. Chatila. Mobile robot navigation: Space modeling and decisional processes. In O. Faugeras and G. Giralt, editors, *Robotics Research 3*. M.I.T. Press, 1986.
- [4] G. Giralt, R. Chatila, and M. Vaisset. An integrated navigation and motion control system for autonomous multisensory mobile robots. In *Robotics Research : The First International Symposium*. MIT Press, Cambridge, Massachusetts, 1984.
- [5] M. Hall. *The Theory of Groups*. Macmillan, 1959.
- [6] R. Hermann and A. J. Krener. Nonlinear controllability and observability. *IEEE Transactions on Circuits and Systems*, AC-22:728-740, 1977.
- [7] A. Isidori. *Nonlinear Control Systems*. Springer-Verlag, 2nd edition, 1989.
- [8] J. Kurzweil and J. Jarnik. Iterated lie brackets in limit processes in ordinary differential equations. *Results in Mathematics*, 14:125-137, 1988.
- [9] G. Lafferriere and H. J. Sussmann. Motion planning for controllable systems without drift. In *Proceedings of the IEEE International Conference on Robotics and Automation*, pages 1148-1153, 1991.
- [10] J.C. Latombe. *Robot Motion Planning*. Kluwer Academic Press, 1991.
- [11] J-P. Laumond. Feasible trajectories for mobile robots with kinematic and environment constraints. In L. O. Hertzberger and F. C. A. Green, editors, *Intelligent Autonomous Systems*, pages 346-354. North Holland, 1987.
- [12] J-P. Laumond. Finding collision-free smooth trajectories for a non-holonomic mobile robot. In *Proceedings of the International Joint Conference on Artificial Intelligence*, pages 1120-1123, 1987.
- [13] J-P. Laumond. Controllability of a multibody mobile robot. In *Proceedings of the International Conference on Advanced Robotics*, pages 1033-1038, Pisa, Italy, 1991.
- [14] J.P. Laumond. Singularities and topological aspects in nonholonomic motion planning. In *Progress in Nonholonomic Motion Planning*. Kluwer Academic Press, 1992.
- [15] J.P. Laumond and T. Siméon. Motion planning for a two degrees of freedom mobile robot with towing. Technical Report 89148, LAAS/CNRS, Toulouse, April 1989.
- [16] Z. Li. *Progress in Nonholonomic Motion Planning*. Kluwer Academic Press, 1992.
- [17] Z. Li and J. Canny. Motion of two rigid bodies with rolling constraint. *IEEE Transactions on Robotics and Automation*, 6(1):62-71, 1990.
- [18] R. M. Murray and S. S. Sastry. Steering nonholonomic systems using sinusoids. In *Proceedings of the IEEE Control and Decision Conference*, pages 2097-2101, 1990.
- [19] R. M. Murray and S. S. Sastry. Steering nonholonomic systems in chained form. In *Proceedings of the IEEE Control and Decision Conference*, pages 1121-1126, 1991.

- [20] H. Nijmeijer and A. J. van der Schaft. *Nonlinear Dynamical Control Systems*. Springer-Verlag, 1990.
- [21] J.P. Laumond P. Jacobs and M. Taix. Efficient motion planners for nonholonomic mobile robots. In *IEEE IROS*, Osaka, November 1991.
- [22] M. Spivak. *A Comprehensive Introduction to Differential Geometry*, volume One. Publish or Perish, Inc., Houston, second edition, 1979.
- [23] H. J. Sussmann. A product expansion for the chen series. In C. I. Byrnes and A. Lindquist, editors, *Theory and Applications of Nonlinear Control Systems*, pages 323–335. North-Holland, 1986.
- [24] H. J. Sussmann and W. Liu. Limits of highly oscillatory controls and the approximation of general paths by admissible trajectories. In *Proceedings of the IEEE Control and Decision Conference*, pages 437–442, 1991.
- [25] H. J. Sussmann and W. Liu. Limits of highly oscillatory controls and the approximation of general paths by admissible trajectories. Technical Report SYCON-91-02, Rutgers Center for Systems and Control, 1991.
- [26] H.J. Sussmann and V. Jurdjevic. Controllability of nonlinear systems. *Journal of Differential Equations*, 12:95–116, 1972.
- [27] D. Tilbury, J-P. Laumond, R. Murray, S. Sastry, and G. Walsh. Steering car-like systems with trailers using sinusoids. In *Proceedings of the IEEE International Conference on Robotics and Automation*, 1992.